ARTICLE

Synthesis of Higher Alcohols from Syngas over Alkali Promoted K-Co-Mo Catalysts Supported on Multi-walled Carbon Nanotubes

Li-li Ji[a], Huan Li[b], Wei Zhang[b], Song Sun[b], Chen Gao[b], Jun Bao[b*], Yun-sheng Ma[a*]

a. Department of Chemical Physics, University of Science and Technology of China, Hefei 230026, China

b. National Synchrotron Radiation Laboratory, University of Science and Technology of China, Hefei 230029, China

(Dated: Received on March 30, 2017; Accepted on April 30, 2017)

A series of carbon nanotubes-supported K-Co-Mo catalysts were prepared by a sol-gel method combined with incipient wetness impregnation. The catalyst structures were characterized by X-ray diffraction, N_2 adsorption-desorption, transmission electron microscopy and H_2-TPD, and its catalytic performance toward the synthesis of higher alcohols from syngas was investigated. The as-prepared catalyst particles had a low crystallization degree and high dispersion on the outer and inner surface of CNTs. The uniform mesoporous structure of CNTs increased the diffusion rate of reactants and products, thus promoting the reaction conversion. Furthermore, the incorporation of CNTs support led to a high capability of hydrogen absorption and spillover and promoted the formation of alkyl group, which served as the key intermediate for the alcohol formation and carbon chain growth. Benefiting from these characteristics, the CNTs supported Mo-based catalyst showed the excellent catalytic performance for the higher alcohols synthesis as compared to the unsupported catalyst and activated carbon supported catalyst.

Key words: CO hydrogenation, Higher alcohol synthesis, Mo-based catalyst, CNTs support

I. INTRODUCTION

Catalytic conversion of the syngas derived from coal, biomass and natural gas into higher alcohols has attracted significant attention because of the scarcity of energy resources, environmental concerns, and gasoline additive octane demands. So far, several catalytic systems have been developed for this reaction during the past few decades [1−3]. Among them, the alkali-promoted Mo-based catalysts are regarded as one of the most promising candidates due to the excellent resistance to sulfur poisoning and coke deposition [4]. Increasing attempts have been made to improve the catalytic performances of Mo-based catalysts. It is found that the 3d transition metals, especially Co, are found to be effective promoters for alkali-promoted Mo-based catalysts, they are known to enhance alcohol production and improve C_{2+} alcohol selectivity. The strong interaction between Co and Mo species is conducive to the formation of higher alcohols.

Catalyst supports have a significant impact on the synthesis of alcohols from syngas. The acid supports such as Al_2O_3 are unfavorable to the synthesis of alcohols because the acidic sites of supports would cause the alcohol dehydration. Activated carbon has the advantages of large surface area, high thermal stability, resistance to acidic or basic media, and shows higher selectivity to alcohols as compared to SiO_2-, Al_2O_3-, and CeO_2-supported catalysts. The interaction between the activated carbon and Mo species plays an important role in the catalytic performance. Our previous study has investigated the activated carbon supported K-Co-Mo catalysts by the synchrotron radiation X-ray absorption fine structure (XAFS). It was found that with an increase in the Mo loading, the surface Mo atoms gradually changed from tetrahedrally coordinated Mo^{6+} species to octahedrally coordinated Mo^{4+}, suggesting a higher reduction degree. The activated carbon supported Mo-based catalyst exhibited an excellent performance for the higher alcohol synthesis, especially the formation of the $C_{2+}OH$.

Multi-walled carbon nanotubes (MWCNTs) have a lot of unique characteristics, such as inert graphitic surface, appropriate pore size distribution, good electrical conductivity and enhanced mass transport capability, which make it a promising support for various catalytic applications [5, 6]. Tavasoli *et al.* [7] found that the CNTs supported Co catalysts showed a higher CO conversion and Fischer-Tropsch synthesis rate than that of the alumina supported catalyst. The reason was attributed that the CNTs aided the uniform dispersion of Co metal clusters on the support. Similar result was re-

*Authors to whom correspondence should be addressed. E-mail: baoj@ustc.edu.cn, ysma@ustc.edu.cn.

ported by Tan *et al*. [8]. They reported a highly dispersed CNT-supported copper-cobalt-cerium catalysts. The employment of CNTs support ensured intimate contact among the metal particles at the nanoscale, which led to a superior selectivity to the ethanol and C_{2+} alcohols. Furthermore, the CNTs can provide the sp^2-C surface-sites for adsorption-activation of H_2 and form a high concentration of H-species micro environment, thereby increasing the hydrogenation reaction rate [9−11]. The uniform pore size distribution of CNTs support exhibited an excellent gas permeability and enabled the metal nanoparticles to be very accessible to the reaction gas, which facilitated the diffusion of the reactants and the dispatched products from the active sites [12].

In our previous work, we have developed a highly homogeneous unsupported K-Co-Mo catalyst prepared by a modified sol-gel method [13] to improve the catalytic performance for higher alcohol synthesis and understand the support effect. Herein, a kind of mesoporous MWCNTs was employed as the support to prepare the K-Co-Mo/CNTs catalysts. The catalyst structures were characterized by a series of physicochemical methods, and the catalytic performance for the synthesis of higher alcohols from syngas was investigated. The relationship between the structure and catalytic performance was also discussed.

II. EXPERIMENTS

A. Catalyst preparation

The CNTs supported K-Co-Mo catalysts (K-Co-Mo/CNTs) were prepared by a sol-gel method combined with incipient wetness impregnation. The MWCNTs with inner diameter of 5−10 nm and outer diameter of 10−20 nm were supplied by Chengdu Institute of Organic Chemistry. Prior to use, the raw CNTs was treated with 30% nitric acid for 24 h, followed by washing with deionized water several times and then drying at 393 K for 12 h. Finally, the CNTs was flushed with pure N_2 at 453 K for 2 h to remove any surface adsorbents. A typical procedure is as follows: firstly, the aqueous solutions of $Co(NO_3)_2{\cdot}6H_2O$, $C_6H_8O_7{\cdot}H_2O$ and K_2CO_3 were added in sequence dropwise to the $(NH_4)_6MoO_{24}{\cdot}4H_2O$ aqueous solution under stirring. The acidity of mixed solution was adjusted to pH=3.5 by adding the ammonia or acetic acid. Subsequently, the mixed solution was kept in a water bath at 343 K until the sol was obtained. The as-prepared sol was then impregnated into CNTs. After ultrasonic dispersion for 1 h, the mixture was dried at 393 K overnight and calcined in flowing nitrogen at 673 K for 4 h. The Mo content in the as-prepared catalysts, expressed as the weight ratio Mo/CNTs, was ranged from 10% to 50%. The atomic ratios of K/Mo and Co/Mo were 0.1 and 0.5, respectively.

B. Catalyst characterization

Powder X-ray diffraction (XRD) patterns were recorded with a Rigaku D/max-γA rotating-anode diffractometer equipped with a Cu Kα radiation source. The BET surface area, pore volume, and pore diameter were determined by nitrogen adsorption at 77 K using a Micromeritics TriStar II 3020 analyzer. Transmission electron microscopy (TEM) was performed using a Philips CM20 (100 kV) transmission electron microscope equipped with a NARON energy-dispersive spectrometer.

The H_2-temperature programmed desorption (H_2-TPD) experiment was carried out on the model of FINESSORB-3013 adsorption instrument. For each experiment, 0.1 g of the sample was packed into a U-type quartz tube. The sample was pretreated under $5\%H_2$/Ar at 798 K for 3 h. After cooling to room temperature, the pretreated sample passed through He atmosphere at 473 K for 0.5 h. Then the pretreated sample was saturated with $5\%H_2$/Ar for 1 h. After that the sample was flushed with heat 373 K for 1 h. Finally the TPD analysis was carried out in a flow of He from 373 K to 1123 K at a heating rate of 10 K/min.

C. Catalytic activity measurements

The catalytic performance of the catalysts for the synthesis of higher alcohols from syngas was tested in a fixed-bed stainless steel reactor with an inner diameter of 8 mm. The reactor was packed with 0.5 g of catalyst that was diluted with quartz sand to produce a total volume of 2 mL and loaded at the center of the reactor tube. Prior to reaction, the catalyst was reduced with $5\%H_2/N_2$ for 12 h at a flow rate of 40 mL/min. After lowered to the reaction temperature, the feed gas containing $V(H_2)$:$V(CO)$:$V(N_2)$=60:30:10 passed through. The effluent gas was cooled in an ice-water bath to separate into gas and liquid phases. Details on the product analytical procedure were described in our previous work [14]. All the activity measurements were performed under the reaction condition of 5.0 MPa, 553 K and gas hourly space velocity (GHSV) 2400 h^{-1}. The activity data were collected after the reaction was performed for 24 h because the alcohol synthesis required an induction period.

III. RESULTS AND DISCUSSION

FIG. 1 shows the XRD patterns of the purified CNTs, the unsupported catalyst and the CNTs supported catalysts with different Mo loading. The purified CNTs showed two broad peaks at 26.1° and 43.2°, respectively. 26.1° corresponding to (002) reflection of graphite and the other small asymmetric peak 43.2° is due to (100) reflection of graphite [15]. For the unsupported cata-

DOI:10.1063/1674-0068/30/cjcp1703061

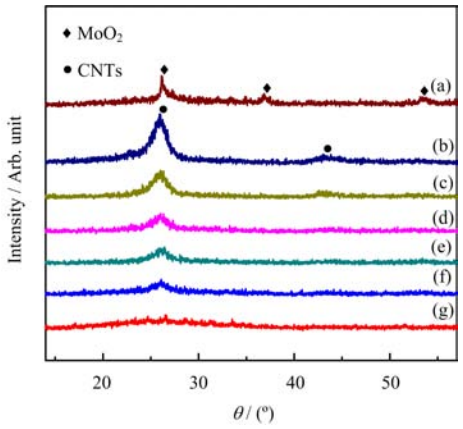

FIG. 1 XRD patterns of (a) unsupported K-Co-Mo, (b) pure CNTs, K-Co-Mo/CNTs with different Mo loading of (c) 10 wt%, (d) 30 wt%, (e) 40 wt%, (f) 50 wt%, and (g) K-Co-Mo/AC with Mo loading of 30 wt%.

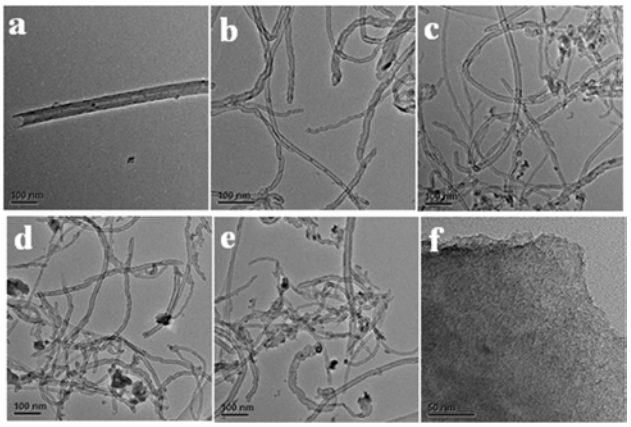

FIG. 2 TEM patterns of the (a) pure CNTs, K-Co-Mo/CNTs with different Mo loading of (b) 10 wt%, (c) 30 wt%, (d) 40 wt%, (e) 50 wt%; and (f) K-Co-Mo/AC with Mo loading of 30 wt%.

lyst, only three wide peaks at 26.1°, 37.0°, and 53.5° were detected, which was assigned to MoO_2. The formation of MoO_2 was attributed to the fact that in nitrogen, the decomposition of citric acid in the sol resulted in the partial reduction of Mo^{+6} species [16]. The supported catalysts exhibited the same diffraction patterns but weaker diffraction intensity as the CNTs support. Besides the CNTs peaks, no peaks assigned to K, Co, or Mo species were detected for the CNTs supported catalysts. Furthermore, with an increase of the Mo contents, the diffraction intensity decreased gradually. The result indicated that the active components had a low degree of crystallization and high dispersion on the surface of CNTs. For comparison, the diffraction pattern of the activated carbon supported catalyst with the Mo/AC ratio of 30% was also presented. Almost no obvious diffraction peaks were observed on the sample.

The TEM images of the sole CNTs and the supported catalysts were shown in FIG. 2. The purified CNTs had open ends with a uniform diameter of about 20 nm, displaying a mesoporous pore structure. For the CNTs supported catalysts, at a low loading of Mo, the catalyst particles were evenly distributed on the CNTs without obvious aggregation. It was noted that some parts of the particles entered the carbon tubes and well dispersed on the inside surface, benefiting from the small particle size and uniform mesoporous structure of CNTs. When the Mo/CNTs weight ratio exceeded 30%, the particles began to aggregate, as shown in FIG. 2 (d) and (e). FIG. 2(f) shows the TEM image of the activated carbon supported catalyst (Mo/AC ratio of 30%). The as-prepared catalyst particles also exhibited a high dispersion on the activated carbon support.

FIG. 3 shows the nitrogen adsorption-desorption isotherms of the pure CNTs and supported K-Co-Mo catalyst. The pure CNTs exhibited a type IV isotherm with a hysteresis loop of type H1 according to the IUPAC classification, and the capillary condensation occurred at a high relative pressure (P/P_0) above 0.80. The result further demonstrated the used CNTs possessed a mesoporous structure with cylindrical pore geometry and a high degree of pore size uniformity, as revealed by the TEM images. The CNTs supported K-Co-Mo catalysts exhibited similar isotherms to that of the purified CNTs, indicating that metal impregnation did not alter the pore structure of the parent support. With an increase of the Mo loading, the BET surface and pore volume (V) of the supported catalysts decreased while the average pore size did not show significant change as shown in Table I. For comparison, the nitrogen adsorption-desorption isotherms of the activated carbon supported K-Co-Mo catalyst with the Mo loading of 30% was also listed (FIG. 3(f)). The adsorption-desorption isotherm showed type I behavior with a H4 type hysteresis loop, indicative of the existence of narrow slit-like pores. Furthermore, a steep increase of adsorbed volume at very low relative pressure, corresponding to micropore volume filling, was observed. The result indicated that the activated carbon supported catalyst contained a certain amount of micropores. Consequently, the catalyst exhibited a much larger BET surface area but smaller pore size as compared to the CNTs supported catalysts with the same composition.

TABLE I Texture properties of the pure CNTs and supported K-Co-Mo catalysts.

Mo/CNTs	$S_{BET}/(m^2/g)$	$V/(cm^3/g)$	D/nm
0	155.73	0.50	12.85
10 wt%	96.07	0.40	16.76
30 wt%	50.01	0.27	16.08
40 wt%	47.16	0.18	15.10
50 wt%	44.09	0.13	14.11
K-Co-Mo/AC	279.96	0.19	2.74

DOI:10.1063/1674-0068/30/cjcp1703061

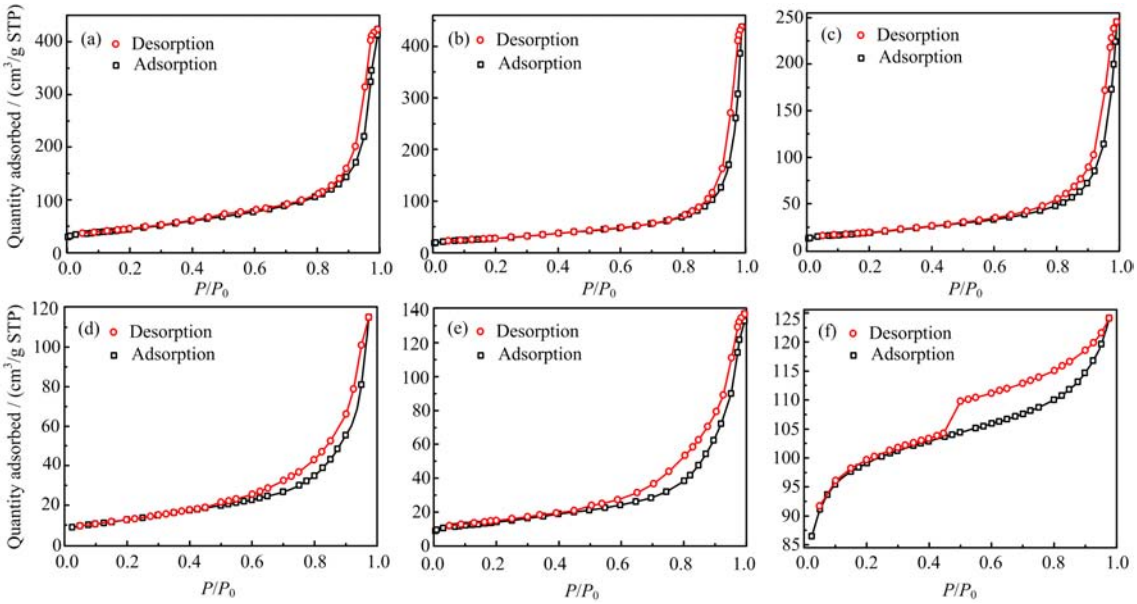

FIG. 3 Nitrogen adsorption-desorption isotherms of (a) pure CNTs, K-Co-Mo/CNTs with different Mo loading of (b) 10 wt%, (c) 30 wt%, (d) 40 wt%, (e) 50 wt%, and (f) K-Co-Mo/AC with Mo loading of 30 wt%.

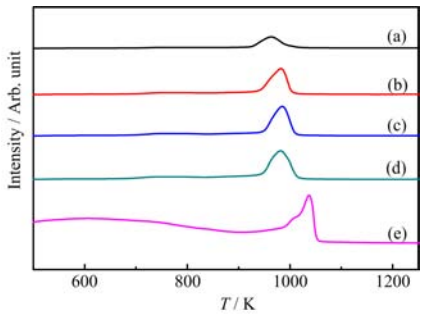

FIG. 4 H_2-TPD of the K-Co-Mo/CNTs with different Mo loading of (a) 10 wt%, (b) 30 wt%, (c) 40 wt%, (d) 50 wt% and (e) K-Co-Mo/AC with Mo loading of 30 wt%.

The hydrogen adsorption and desorption ability of the catalysts are investigated by H_2-TPD experiments and the profiles were shown in FIG. 4. The CNTs supported catalysts exhibited a predominant peak of hydrogen desorption at 973 K. Besides, a very weak wide peak appeared around 740 K. The weak desorption peak was most probably due to the molecularly adsorbed hydrogen. The strong peak was attributed to the dissociatively chemisorbed hydrogen, which was suggested to have a significant impact on the catalytic activity. The capacity of adsorbing hydrogen increased with an increase of the Mo loading and reached the highest level at the Mo loading of 30%. With a further increase of the Mo loading, the adsorption capacity of hydrogen did not show significant change. The H_2-TPD profile of the activated carbon supported K-Co-Mo catalyst (Mo/AC ratio of 30%) was also listed. The sample exhibited a stronger low temperature desorption peak than that of the CNTs catalysts, which may be due to the fact that the presence of the micropores in the activated carbon was conducive to the absorption of molecular hydrogen. It was noted that its peak corresponding to dissociatively chemisorbed hydrogen shifted to higher temperature as compared to the CNTs catalyst, indicative of a stronger interaction between the chemisorbed H-species and activated carbon support. Furthermore, a shoulder peak was also observed, which may be attributed that the non-uniformly distributed pore size of activated carbon resulted in a different diffusion rate of H-species.

Table II lists the catalytic performance of the K-Co-Mo/CNTs catalysts for the synthesis of higher alcohols. For comparison, the unsupported catalyst was also tested under the same conditions. The unsupported K-Co-Mo exhibited a relative low activity toward alcohol synthesis, and the predominant alcohol product was methanol. The incorporation of CNTs support led to a significant increase in the alcohol production. As shown in Table II, the catalyst with a Mo/CNTs weight ratio of 30% showed the best catalytic performance for alcohols synthesis. The STY of total alcohols was 141.7 $g{\cdot}kg^{-1}{\cdot}h^{-1}$, about 9 times as high as that of the unsupported sample and the alcohol selectivity increased from 9.5% to 35.4%. In particular, the methanol production was inhibited remarkably. The effect of the H_2/CO ratio on the catalyst activity was also investigated. When the H_2/CO ratio decreased from 2 to 1, the catalyst with a Mo/CNTs weight ratio of 30% alcohol selectivity and $C_{2+}OH/MeOH$ ratio further increased up to 49.8% and 2.33, respectively. The ethanol became the predominant alcohol product. Meanwhile, the alcohol STY still reached 110.0 $g{\cdot}kg^{-1}{\cdot}h^{-1}$. The

DOI:10.1063/1674-0068/30/cjcp1703061

TABLE II Catalytic performance toward alcohol formation from syngas over the catalysts. Alc. Sel. is calculated on a CO_2-free basis, Reaction conditions are 553 K, 5.0 MPa, 2400 h^{-1}. CO conv., Alc. Sel., and C_nOH Sel. in C-mol%, Alc. STY in $g{\cdot}kg^{-1}{\cdot}h^{-1}$

Mo/CNTs	CO conv.		H_2/CO	Alc. Sel.	Alc. STY	C_nOH Sel.				$C_{2+}OH$/MeOH
	ROH+HC	CO_2				MeOH	EtOH	PrOH	BuOH	
K-Co-Mo	17.5	14.5	2	9.5	15.7	3.1	1.9	1.3	0.4	1.16
10 wt%	18.4	11.7	2	49.6	90.9	17.0	18.4	10.9	3.3	1.92
30 wt%	34.1	28.1	2	35.4	141.7	12.5	12.1	8.2	2.6	1.85
40 wt%	39.5	29.6	2	29.7	111.7	10.2	10.2	7.1	2.3	1.92
50 wt%	34.3	27.5	2	30.0	110.2	10.7	10.8	7.2	2.3	1.92
30 wt%	9.68	17.6	1	49.8	110.0	14.9	18.7	12.1	4.1	2.33
K-Co-Mo/AC	5.34	7.21	1	54.9	68.5	17.9	21.0	12.4	3.6	2.08

presented activity data are encouraging because they were tested under very mild conditions of 5.0 MPa and 2400 h^{-1}. The decrease of H_2/CO ratio improved the alcohol selectivity, especially the formation of $C_{2+}OH$. The reason was attributed that increasing the CO concentration decreased the relative rate of hydrogenation of the methanol precursor and thus inhibited the synthesis of methanol. The formation of higher alcohols appeared to be a slow step relative to the rate of hydrogenation of methanol precursor [17]. In addition, increasing the CO concentration also favored the insertion of CO into an alkyl group to form the acyl species, which was regarded as the key intermediate for the synthesis of alcohols [18]. The CO_2 was yielded from the water-gas-shift (WGS) side reaction. No significant change in CO_2 production was observed when the Mo/CNTs weight ratio increased from 30% to 50%. For comparison, the catalytic performance of the activated carbon supported K-Co-Mo catalyst (Mo loading of 30%) was tested under the same conditions. In comparison to the activated carbon sample, the alcohol selectivity over the CNTs catalyst showed a slight decrease, while the alcohol STY increased more than 60%. In particular, the $C_{2+}OH$/MeOH ratio also increased from 2.08 to 2.33. The results indicated the CNTs supported K-Co-Mo catalyst exhibited better catalytic performance for the higher alcohol synthesis, although its BET surface area was much lower than that of the activated carbon sample.

The support properties, such as acidity, components dispersion, and pore structure *etc.*, have a significant impact on the catalytic performance for alcohols synthesis from syngas. The CNTs and activated carbon are the neutral carbon materials. The as-prepared K-Co-Mo catalysts supported on the CNTs and activated carbon exhibited a low crystallization degree and high dispersion, as revealed by the XRD and TEM results. This suggested that the supported catalysts had a high active surface area, which contributed to higher activity compared to the unsupported catalyst.

The pore structure of the support significantly affected the catalytic activity for CO hydrogenation, especially the product distribution. Small pore size will result in poor intra-pellet diffusion efficiencies of molecules. Slow transport of reactants to, and products from, active sites often inhibits the reaction rate and affects the product selectivity. For the higher alcohol synthesis from syngas, Surisetty *et al.* have investigated the influence of porous characteristics of support and concluded that the mesoporous support was conducive to the alcohol production, especially the formation of $C_{2+}OH$ [19]. The hydrogen dissociation and spillover capability also play an important role in the CO hydrogenation reaction. The formation of higher alcohols from syngas over the Mo-based catalyst follows a CO insertion mechanism [20]. The dissociated H-species reacts with the dissociated CO to form the alkyl group. The non-dissociatively CO insertion to the alkyl group forms the alcohol product. The alkyl group serves as the key intermediate for alcohol formation and carbon chain growth. The nitrogen adsorption-desorption isotherms and TEM images showed that the CNTs supported catalysts possessed a uniform mesoporous structure. This meant that catalyst had a higher diffusion efficiencies of molecule and increased reaction rate as compared to the activated carbon support containing micropores. Furthermore, the H_2-TPD result revealed that the CNTs catalyst had a strong adsorption capacity of hydrogen and relatively weaker interaction with the H-species compared to the activated carbon catalyst. The reason may be attributed that the surface sp^2-C sites of CNTs promoted the adsorption and activation of hydrogen [21]. The weak interaction between the H-species and catalyst indicated a higher spillover capability of H-species, which was conducive to the formation of alkyl group intermediate and thus promoted the alcohol production. These factors were suggested to be responsible for the excellent catalytic performance of the CNTs supported K-Co-Mo catalysts for the higher alcohol synthesis from syngas.

IV. CONCLUSION

Multi-walled carbon nanotubes supported K-Co-Mo catalyst was prepared by a sol-gel method. The K-Co-

DOI:10.1063/1674-0068/30/cjcp1703061

Mo/CNTs catalyst showed a much higher activity for the synthesis of higher alcohols than that of the unsupported catalyst and activated carbon supported catalyst. The enhanced performance can be attributed to the fact that the CNTs supported catalyst had a low crystallization degree and high dispersion, which suggested a high active surface area. The uniform mesoporous structure of CNTs support led to a high diffusion efficiencies of molecule and increased conversion rate. Furthermore, the CNTs catalyst had a strong capability of hydrogen absorption and spillover, which was conducive to the formation of alkyl group intermediate and thus enhanced the alcohol production.

V. ACKNOWLEDGMENTS

This work was supported by National Natural Science Foundation of China (No.21673214).

[1] J. Bao, Y. L. Fu, Z. H. Sun, and C. Gao, Chem. Commun. 746 (2003).
[2] V. Mahdavi, M. H. Peyrovi, M. Islami, and J. Y. Mehr, Appl. Catal. A **281**, 259 (2005).
[3] R. Burch and M. J. Hayes, J. Catal. **165**, 249 (1997).
[4] S. Zaman and K. J. Smith, Catal. Rev. **54**, 41 (2012).
[5] P. Serp, M. Corrias, and P. Kalck, Appl. Catal. A **253**, 337 (2003).
[6] X. L. Pan, Z. L. Fan, W. Chen, Y. J. Ding, H. Y. Luo, and X. H. Bao, Nat. Mater. **6**, 507 (2007).
[7] A. Tavasoli, R. M. M. Abbaslou, M. Trepanier, and A. K. Dalai, Appl. Catal. A **345**, 134 (2008).
[8] P. Wang, J. F. Zhang, Y. X. Bai, H. Xiao, S. P. Tian, H. J. Xie, G. H. Yang, N. Tsubaki, Y. Z. Han, and Y. S. Tan, Appl. Catal. A **514**, 14 (2016).
[9] X. M. Wu, Y. Y. Guo, J. M. Zhou, G. D. Lin, X. Dong, and H. B. Zhang, Appl. Catal. A **340**, 87 (2008).
[10] C. H. Ma, H. Y. Li, G. D. Lin, and H. B. Zhang, Appl. Catal. B Environ. **100**, 245 (2010).
[11] W. Feng, Q. W. Wang, B. Jiang, and P. J. Ji, Ind. Eng. Chem. Res. **50**, 11067 (2011).
[12] M. Khavarian, S. P. Chai, and A. R. Mohamed, Fuel **158**, 129 (2015).
[13] J. Bao, Y. L. Fu, and G. Z. Bian, Catal. Lett. **121**, 151 (2008).
[14] M. M. Lv, W. Xie, S. Sun, G. M. Wu, L. R. Zheng, S. Q. Chu, C. Gao, and J. Bao, Catal. Sci. Technol. **5**, 2925 (2015).
[15] I. Eswaramoorthi, V. Sundaramurthy, and A. K. Dalai, Appl. Catal. A **313**, 22 (2006).
[16] J. Bao, Z. H. Sun, Y. L. Fu, G. Z. Bian, Y. Zhang, and N. Tsubaki, Top Catal. **52**, 789 (2009).
[17] E. Tronconi, N. Ferlazzo, P. Forzatti, and I. Pasquon, Ind. Eng. Chem. Res. **26**, 2122 (1987).
[18] A. Muramatsu, T. Tatsumi, and H. Tominaga, J. Phys. Chem. **96**, 1334 (1992).
[19] V. R. Surisetty, A. K. Dalai, and J. Kozinski, Appl. Catal. A **393**, 50 (2011).
[20] A. Muramatsu, T. Tatsumi, and H. Tominaga, J. Phys. Chem. **96**, 1334 (1992).
[21] J. J. Wang, J. R. Xie, Y. H. Huang, B. H. Chen, G. D. Lin, and H. B. Zhang, Appl. Catal. A **468**, 44 (2013).

DOI:10.1063/1674-0068/30/cjcp1703061